

## Separation of strain and quantum-confinement effects in the optical spectra of quantum wires

E. Martinet, M.-A. Dupertuis, F. Reinhardt, G. Biasiol, and E. Kapon

*Department of Physics, Swiss Federal Institute of Technology Lausanne, CH-1015 Lausanne EPFL, Switzerland*

O. Stier, M. Grundmann, and D. Bimberg

*Institute für Festkörperphysic, Technische Universität Berlin, Hardenbergstraße 36, D-10623 Berlin, Germany*

(Received 30 June 1999)

The photoluminescence (PL) and PL-excitation (PLE) spectra of  $\text{In}_y\text{Ga}_{1-y}\text{As}/\text{Al}_x\text{Ga}_{1-x}\text{As}$  compressively strained V-groove quantum wires (QWR's) are compared to that of lattice-matched  $\text{GaAs}/\text{Al}_y\text{Ga}_{1-y}\text{As}$  QWR's with the same wire geometry. The PL is preferentially polarized along the QWR axis and the PL anisotropy increases with increasing indium content  $y$ . The observed PLE anisotropy also increases with  $y$  at the ground subband transition but is nearly independent of excited subband indices, unlike the case of lattice-matched QWR's. We calculated the absorption spectra of the QWR's using an  $8 \times 8$   $\mathbf{k} \cdot \mathbf{p}$  model to separate the effects of quantum confinement (QC) and strain on the valence-band (VB) mixing. The modification of the optical anisotropy is explained by the strain-induced decoupling of the heavy-hole and light-hole subband edges, lifting the strong VB mixing observed in the  $\text{GaAs}/\text{Al}_x\text{Ga}_{1-x}\text{As}$  case. The subband separation energies are, however, nearly unaffected by the strain as they are mainly governed by QC effects in the conduction band.

The introductions of strain<sup>1</sup> and low-dimensional quantum confinement<sup>2</sup> (QC) have been shown to be important means for tailoring the optical properties of advanced semiconductor structures. Strained nanostructures have been reported to be useful for quantum wire (QWR) lasers<sup>3</sup> and the self-organized growth of quantum dot (QD) arrays.<sup>4</sup> However, it has only been recently that the interplay between strain and dimensionality effects in QWR and QD systems has been given consideration.<sup>5-9</sup> Polarization analysis of the optical spectra has been one of the main techniques used to estimate the extent of QC in lattice matched QWR's.<sup>10,11</sup> In such structures, the valence-band-(VB-) mixing effects are primarily governed by the one-dimensional (1D) confinement.<sup>11</sup> As strain also alters the symmetry of the VB-edge states, the optical anisotropy in strained QWR systems is determined by the relative weight of strain and quantum-confinement effects.<sup>8,9,12</sup> Large photoluminescence (PL) anisotropy, with preferential emission along the QWR axis, has been reported for QWR arrays formed by strain-induced mechanisms such as lateral ordering of alloy<sup>13</sup> or stressor patterning.<sup>14,15</sup> However, a clear separation of QC and strain effects was not possible in such structures as the lateral confinement potential was determined by the strain itself. Notomi *et al.*<sup>6</sup> have demonstrated the effect of dimensionality in strained rectangular QWR realized by the etch and regrowth process, and analyzed the relative weight of strain and QC at the band-edge transition using magneto-PL experiments.<sup>8</sup> Gershoni *et al.*<sup>14</sup> have observed a clear anisotropy of the PL-excitation (PLE) spectra of QWR's resulting from the growth of a quantum well (QW) on the cleaved edge of a strained superlattice.<sup>14</sup> In this case, the anisotropy was explained by the combined effects of the band warping, and the strain-induced shallow confinement. On the other hand, seeded self-ordering of lattice-matched and strained layers on V-grooved GaAs substrates has been demonstrated to yield a good control of the QWR geometry, together with large con-

finement potentials.<sup>11,16,17</sup> Vouilloz *et al.*<sup>11</sup> have identified the effects of the QC on the VB mixing in the excitation spectra of lattice-matched  $\text{GaAs}/\text{Al}_y\text{Ga}_{1-y}\text{As}$  V-groove QWR's.<sup>11</sup> In a previous paper, we have shown that the shape of such QWR's is nearly unaffected when a pseudomorphic  $\text{In}_y\text{Ga}_{1-y}\text{As}$  layer ( $y < 0.3$ ) is introduced in the QWR's.<sup>17</sup> Therefore, it should be possible to isolate the impact of pure strain effects on the excitation spectra of such strained V-groove QWR's. In the present paper, we report on the direct observation of the strain-induced modifications of the VB mixing at the ground and excited subband transitions of  $(\text{In})\text{GaAs}/\text{Al}_y\text{Ga}_{1-y}\text{As}$  V-groove QWR's. The anisotropy in the excitation spectra of the strained wires increases with increasing strain at the band edge but is nearly independent of the excited transition indices, in strong contrast to what is observed for the lattice-matched QWR's. On the other hand, the subband separation energy is nearly unaffected by the presence of indium in the QWR. The PLE spectra are compared to an  $8 \times 8$   $\mathbf{k} \cdot \mathbf{p}$  calculation of the polarized absorption spectra taking into account VB-mixing effects. The 1D transition energy spacing is shown to be governed by QC effects in the conduction band while the modifications in the optical anisotropy result from the shear-strain induced decoupling of the heavy-holes (hh) and light-holes (lh) subbands.

A series of  $\text{In}_y\text{Ga}_{1-y}\text{As}/\text{Al}_{0.27}\text{Ga}_{0.73}\text{As}$  QWR's were grown at 650 °C by low-pressure organometallic chemical vapor deposition on (001) GaAs substrates patterned with 3- $\mu\text{m}$  pitch  $[1\bar{1}0]$ -oriented corrugations (wires oriented in the  $[1\bar{1}0]$  direction). We consider here three samples resulting from the deposition on 3- $\mu\text{m}$  pitch V-grooved substrates of a pseudomorphic strained film with  $y=0, 0.08$  or  $0.15$ , and a nominal thickness of 3 nm. A detailed description of the resulting crescent-shaped, strained-QWR geometry can be found elsewhere.<sup>17</sup>

The samples were mounted in a helium-flow cryostat and kept at a temperature of 12 K. The optical spectra were ob-

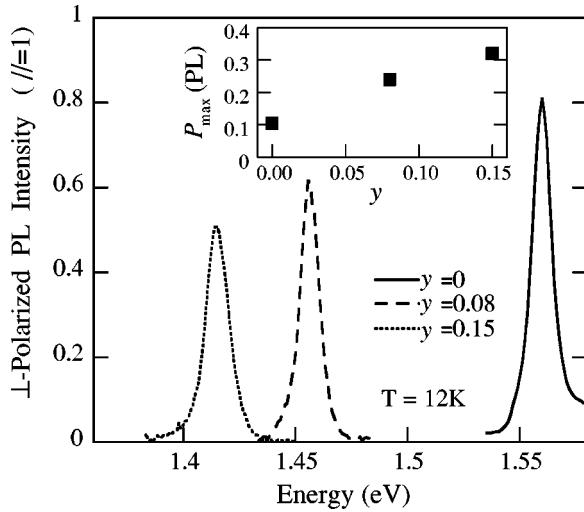


FIG. 1. QWR photoluminescence (PL) spectra vs In mole fraction with polarization perpendicular to the QWR (polarization along the QWR normalized to 1). Inset: degree of linear polarization  $P_{max}$  versus the In mole fraction.

tained using light from an argon-ion laser (2.4 eV) for PL experiments and from a titanium-sapphire laser for the PLE experiments, with an excitation spot size of about 50  $\mu\text{m}$ . Typical power densities of 20  $\text{W}/\text{cm}^2$  were used. The emission was detected using a photomultiplier tube for the lattice-matched QWR sample and using a germanium detector with a lock-in technique for the strained QWR samples. The different peaks in the PL spectra, arising from different regions in the samples, were identified by spatially resolved cathodoluminescence.<sup>17</sup> The samples were then selectively etched and the sidewall and ridge QW regions were removed. The linearly polarized PL and PLE spectra were measured in a pseudobackscattering geometry from the (001) plane, with the polarization either parallel ( $\parallel$ ,  $[1\bar{1}0]$  direction) or perpendicular ( $\perp$ ,  $[110]$  direction) to the wire axis. We define the degree of linear polarization of the PL and PLE spectra, henceforward called “optical anisotropy,” as  $P = (I_{\parallel} - I_{\perp}) / (I_{\parallel} + I_{\perp})$ , where the intensities refer to the linearly polarized PL or PLE intensities, respectively. Small extrinsic electromagnetic effects could have resulted from the remaining shallow surface corrugations of our samples after etching.<sup>11,18</sup> However, the comparison of the optical anisotropy of selectively-etched QWR samples with that of planarized QWR samples allowed us to rule out such effects in our spectra.

Figure 1 shows the  $\perp$ -polarized PL spectra of the QWR samples normalized to the  $\parallel$ -polarized PL intensity at the corresponding QWR peak. The emission is always preferentially polarized along the wire axis ( $P > 0$ ). We also find that the PL anisotropy  $P$  varies across the emission line, with a maximum that is blueshifted as compared to the PL peak. When the indium concentration is increased, this blueshift is increased from 10 meV ( $y=0$ ) to 14 meV ( $y=0.15$ ). The inset in Fig. 1 shows the evolution of the maximum PL anisotropy  $P_{max}$  as a function of the indium composition. An increase in  $P_{max}$  is observed, from 0.11 ( $y=0$ ) to 0.31 ( $y=0.15$ ). A similar variation of the anisotropy across the emission line has been observed in the case of lattice-matched QWR's and attributed to exciton localization

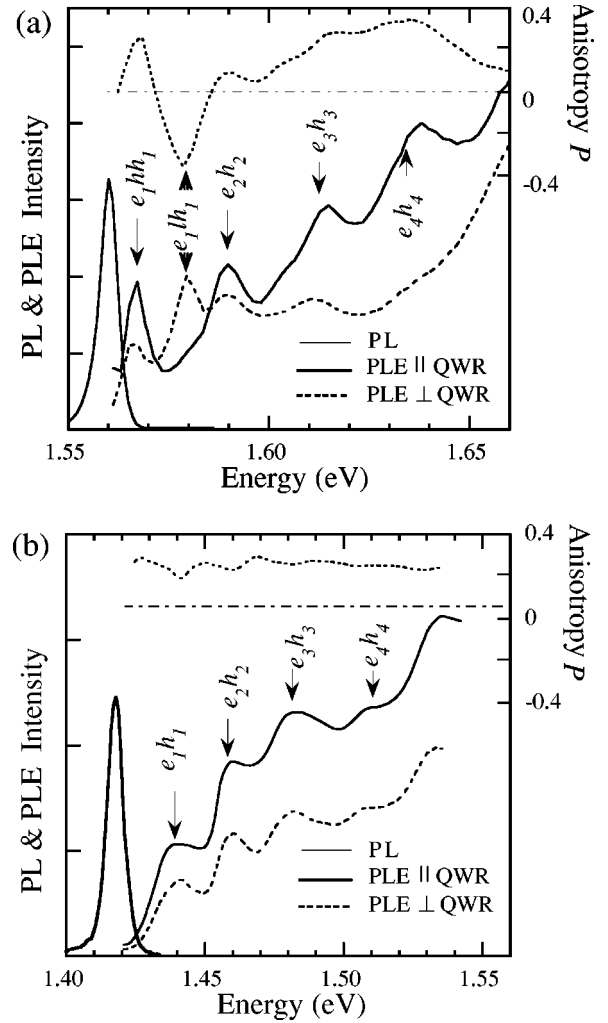


FIG. 2. Photoluminescence (PL), PL-excitation (PLE), and PLE anisotropy ( $P$ ) spectra of the lattice-matched reference QWR (a) and strained QWR (b) samples. The arrows indicate the calculated transition energies.

effects.<sup>11</sup> The increase in the observed blueshift with increasing  $y$  can be explained by larger interface roughness in the strained QWR's due to the larger  $\text{In}_y\text{Ga}_{1-y}\text{As}$  alloy disorder and/or larger nonuniformities along the axis of the QWR's.<sup>17</sup> However, the increase of  $P_{max}$  with indium composition cannot be explained by such localization effects as these tend to depolarize the emission,<sup>11</sup> but is rather to be attributed to the increase in the intrinsic anisotropy of the optical matrix elements at the ground-state transition of the QWR's.<sup>11</sup>

Unlike for the PL, localization effects should play a marginal role in optical-absorption spectra as the density of states is governed by extended QWR states.<sup>11</sup> In order to identify the effects of strain and QC on the absorption anisotropy at the ground and excited QWR states, we have compared the linearly polarized PLE spectra of the QWR samples with  $y=0$  and 0.15. The PLE spectra were detected at the peak of the QWR PL. Figure 2 shows the unpolarized PL and the polarized PLE spectra for  $\parallel$  (full line) and  $\perp$  (dashed lines) polarizations of the GaAs QWR (a) and  $\text{In}_y\text{Ga}_{1-y}\text{As}$  QWR (b) samples. The  $\parallel$ -polarized PLE spectrum of the GaAs QWR shows more than five narrow sub-band peaks [full width at half maximum (FWHM) is 8 meV]

identified as the  $e_n$ - $hh_n$  transitions.<sup>11</sup> The first subband separation energies are measured to be  $\sim 23$  meV. More than five subband transitions are also observed in the  $\parallel$ -polarized PLE spectrum of the strained QWR's, with separation energies ranging from 22 to 26 meV. A larger subband linewidth ( $\sim 12$  meV) than that of the GaAs QWR is observed. Such an increase is consistent with that observed in the PL linewidth and the measured PLE Stokes shifts [14 meV ( $y=0.15$ ), 9 meV ( $y=0$ )]. However, a large difference is observed in the  $\perp$ -polarized PLE spectra and resulting PLE anisotropy,  $P$  [dotted lines in Figs. 2(a) and 2(b)]. The  $\perp$ -polarized PLE spectrum of the lattice-matched QWR's shows an extra feature between the first two subband transitions which is attributed to the transition between the electron and quasi-light-hole ground states ( $e_1$ - $lh_1$ ).<sup>11</sup> Such a feature is absent in the  $\perp$ -polarized PLE spectrum of the strained QWR's. The PLE anisotropy measured at the fundamental subband transition is increased from  $P=0.26$  ( $y=0$ ) to 0.29 for  $y=0.15$ . Moreover, the PLE anisotropy of the strained QWR is shown to be weakly dependent on subband indices ( $0.26 \leq P \leq 0.30$  for  $1 \leq n \leq 5$ ). It is even smaller than that of the lattice-matched QWR at some of the higher excited subband transitions, e.g.,  $e_4$ - $hh_4$ .

For a quantitative understanding of the optical spectra of the lattice-matched QWR, we have used a  $4 \times 4$   $\mathbf{k} \cdot \mathbf{p}$  Luttinger model to describe the VB-mixing effects arising from the 1D QC.<sup>11</sup> The QWR interface profile is measured on transmission electron microscope (TEM) micrographs. Excitonic effects are not included. A good agreement is found between the experimental PLE spectra and the calculated absorption spectra. The calculated transition energies are indicated with arrows on Fig. 2(a), after a rigid energy shift accounted for the excitonic binding energy. The absorption spectra for  $\parallel$  polarization show resonances at the  $e_n$ - $lh_n$  transitions with  $1 \leq n \leq 4$ . The calculated separation energy between the first subband transitions is 25 meV. The absorption spectrum for the  $\perp$ -polarization shows a preferential coupling to the  $e_1$ - $h_6$  transition. This corresponds to the sign reversal in the anisotropy spectrum [dotted line in Fig. 2(a)]. The hole state involved in the transition is shown to have the character of a ground light-hole (lh), with a degree of light-hole character of 0.71, as defined in Ref. 11. The discrepancy between the calculated (0.32) and the measured band-edge anisotropies [0.10 (PL) and 0.26 (PLE)] can be explained by localization effects and the absence of excitonic effects in our model.

Before separating the weights of the strain and the QC in the excitation spectra of the  $\text{In}_y\text{Ga}_{1-y}\text{As}$  QWR's, we have first evaluated the consequences of the slightly different QWR shapes between the strained and the lattice-matched QWR samples considered here. Slightly wider wire facets were observed in the TEM micrographs of the strained QWR's, resulting in a slightly larger central thickness at the center of the crescent [10.2 nm ( $y=0.15$ ) versus 9.6 nm ( $y=0$ )].<sup>17</sup> We have then calculated the absorption spectra of an ideal lattice-matched GaAs QWR having the interface profile of the strained  $\text{In}_y\text{Ga}_{1-y}\text{As}$  QWR's. The calculated absorption spectra of such an ideal QWR showed a 7-meV redshift of the ground subband transition and subband spacings nearly unaffected by the difference in shapes (23 meV, as compared to 25 meV for the GaAs real QWR's). Figure 3

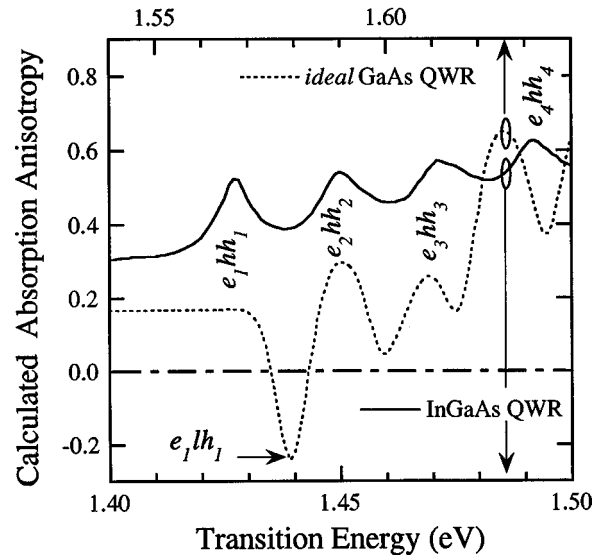


FIG. 3. Calculated relative anisotropy of absorption for strained (a) and a model GaAs QWR with same potential profile (b).

shows the calculated optical anisotropy of the ideal lattice-matched QWR (dashed line). The absorption anisotropy of this GaAs QWR is very similar to the measured [Fig. 2(a)] and calculated anisotropies of the real lattice-matched QWR's.

An  $8 \times 8$   $\mathbf{k} \cdot \mathbf{p}$  Luttinger model was then used to calculate the band structure of the real strained QWR, including the VB-mixing effects.<sup>7</sup> The strain distribution in and around the QWR's is calculated by minimizing the total strain energy of the structure using elastic continuum theory. We assumed that the In composition throughout the QWR was uniform and equal to the nominal value ( $y=0.15$ ).<sup>7</sup> Excitonic effects are not considered. The absorption spectra were computed assuming a dispersion up to  $k_{max}=0.3$   $\text{nm}^{-1}$ , and a homogeneous broadening of  $\gamma=7.5$  meV (Lorentzian FWHM). The calculated transition energies are indicated by arrows in Fig. 2(b). The calculated subband spacing (24 meV) is nearly equal to the measured one. The calculated anisotropy  $P$  of the absorption spectra for the  $\text{In}_y\text{Ga}_{1-y}\text{As}/\text{Al}_y\text{Ga}_{1-y}\text{As}$  QWR sample is shown in Fig. 3 (solid line). A good qualitative agreement is found between the anisotropy of the measured PLE and calculated absorption spectra for all subband transitions. The measured anisotropy at the band edge [0.29 (PLE)], is consistent with the calculated one (0.31). It is increased due to the strain from 0.18 (due to pure QC effects) in the lattice-matched QWR. Moreover, such an anisotropy is weakly dependent on the subband transition indices. Both effects can be explained as the result of the strain distribution.<sup>5</sup> The small discrepancy with  $P$  observed at the peaks can be explained by broadening effects and the absence of excitonic effects in our calculation.

A simple two-dimensional (2D) strained-QW model can be useful for understanding the origin of such an effect in the shear components of the strain.<sup>16</sup> The otherwise degenerate bulk band edges for heavy and light holes are split due to the shear strain: this VB splitting is about 80 meV for  $y=0.15$ . The consequence is that the first possible transition with a quasi-lh state is shifted away from the band edge by more than five electronic subband separation energies ( $\sim 24$

meV). This removal of VB-mixing effects between light- and heavy-hole states is responsible for the absence of large variations (namely a sign reversal) in the anisotropy spectrum of the strained QWR's. We can also explain the negligible variation of the transition energy spacing between the strained and a lattice-matched QWR's by considering this simple 2D model. The QC of electrons give  $\sim 80\%$  of the transition spacings. It is sensitive to the indium composition through the modifications of the confinement potential and is only marginally affected by the strain itself. The absence of variation in the subband spacings is explained by the balance between the larger quantum confinement [smaller electron masses ( $\sim 14\%$ ) and deeper confinement potential ( $\sim 40\%$ )] and the slightly wider QWR geometry.

In conclusion, the polarization dependence of the absorption coefficient for compressively strained V-groove QWR's was investigated as a function of strain. The linearly polarized photoluminescence (PL) and PL-excitation (PLE) spectra were measured for a series of QWR's with  $y=0$  and 0.15. We have clearly separated the QC and strain effects in

their emission and absorption spectra. The subband separation energy is weakly affected by strain and is mainly governed by QC effects in the conduction band resulting from the crescent-shaped QWR profile. The polarization anisotropy at the band-edge transition observed in PL and PLE is increasing with indium composition due to the modification of the hole symmetry under strain. However, in contrast to the lattice-matched case, the PLE intensity of the strained QWR's is nearly independent on transition indices. This is explained by the shear-strain induced splitting of the hh and lh bulk valence bands resulting in a large decoupling of hh and lh subbands. This tuning of the strain and confinement properties should be useful for optimizing the polarization properties of strained-QWR devices.<sup>3,19</sup>

We thank C. Constantin, H. Weman, F. Vouilloz, D. Oberli, and A. Sadeghi for experimental assistance or fruitful discussions. This work was supported by the Swiss National OPTIQUE II Priority Program.

- 
- <sup>1</sup>*Strained-Layer Superlattices*, edited by T.P. Pearsall, Semiconductors and Semimetals Vol. 32 (Academic, New York, 1990).
- <sup>2</sup>Y. Arakawa and H. Sakaki, *Appl. Phys. Lett.* **40**, 939 (1982).
- <sup>3</sup>M. Walther, E. Kapon, C. Caneau, D.M. Hwang, and L.M. Schiavone, *Appl. Phys. Lett.* **62**, 2170 (1993); S. Tiwari, G.D. Pettit, K.R. Milkove, F. Legoues, R.J. Davis, and J.M. Woodall, *ibid.* **64**, 3536 (1994).
- <sup>4</sup>D. Leonard, M. Krishnamurthi, C.M. Reaves, S.P. Denbaars, and P.M. Petroff, *Appl. Phys. Lett.* **63**, 3203 (1993).
- <sup>5</sup>M. Grundmann, O. Stier, and D. Bimberg, *Phys. Rev. B* **50**, 14 187 (1994).
- <sup>6</sup>M. Notomi, J. Hammersberg, H. Weman, S. Nojima, H. Sugiura, M. Okamoto, M. Tamamura, and M. Potemki, *Phys. Rev. B* **52**, 11 147 (1995).
- <sup>7</sup>O. Stier and D. Bimberg, *Phys. Rev. B* **55**, 7726 (1997).
- <sup>8</sup>M. Notomi, J. Hammersberg, J. Zeman, H. Weman, M. Potemki, H. Sugiura, and T. Tamamura, *Phys. Rev. Lett.* **80**, 3125 (1998).
- <sup>9</sup>M. Grundmann, O. Stier, and D. Bimberg, *Phys. Rev. B* **52**, 11 969 (1995).
- <sup>10</sup>H. Akiyama, T. Someya, and H. Sakaki, *Phys. Rev. B* **53**, R4229 (1996).
- <sup>11</sup>F. Vouilloz, D. Y. Oberli, M.A. Dupertuis, A. Gustafsson, F. Reinhardt, and E. Kapon, *Phys. Rev. Lett.* **78**, 1580 (1997); *Phys. Rev. B* **57**, 12 378 (1997).
- <sup>12</sup>I. Vurgaftman and J. Singh, *J. Appl. Phys.* **77**, 4931 (1995).
- <sup>13</sup>P. Dua, S.L. Cooper, A.C. Chen, and K.Y. Cheng, *Appl. Phys. Lett.* **69**, 2262 (1996).
- <sup>14</sup>D. Gershoni, J.S. Weiner, A.S.N.G. Chu, G.A. Baraff, J.M. Vandenberg, L.N. Pfeiffer, K. West, R.A. Logan, and T. Tanbun-Ek, *Phys. Rev. Lett.* **65**, 1631 (1990).
- <sup>15</sup>K. Kash, J.M. Worlock, A.S. Gozdz, B.P. Van der Gaag, J.P. Harbison, P.S.D. Lin, and L.T. Florez, *Surf. Sci.* **229**, 245 (1990).
- <sup>16</sup>M. Grundmann, J. Christen, D. Bimberg, and E. Kapon, *J. Non-linear Opt. Phys. Mater.* **4**, 99 (1995).
- <sup>17</sup>E. Martinet, F. Reinhardt, A. Gustafsson, G. Biasiol, and E. Kapon, *Appl. Phys. Lett.* **72**, 701 (1998).
- <sup>18</sup>U. Bockelmann, *Europhys. Lett.* **16**, 601 (1991).
- <sup>19</sup>C. Constantin, E. Martinet, A. Rudra, and E. Kapon, *Phys. Rev. B* **59**, R7809 (1999).